Control laws for a formation of autonomous flight vehicles

M. Chiaramonti and G. Mengali
g.mengali@ing.unipi.it
Department of Aerospace Engineering
University of Pisa
Pisa, Italy

ABSTRACT

This paper investigates the performance of a flight control system, based on nonlinear dynamics inversion theory, whose aim is to maintain a given geometry of a formation of unmanned aerial vehicles. A fundamental aspect is the complete three dimensionality of the formation geometry that provides a substantial improvement over existing two-dimensional control laws. The designed control system has been implemented in a Simulink® environment and its effectiveness has been tested with a campaign of numerical simulations.

NOMENCLATURE

$\bar{c}$	mean aerodynamic chord
c_i	coefficient
h	height
k	transfer function gain
m	aircraft mass
p	roll rate
q	pitch rate
r	yaw rate
s	Laplace variable
T	thrust
$\mathbf{u}$	intermediate input vector
V	aircraft velocity
x	longitudinal component of aircraft position
$\mathbf{x}$	state vector
y	lateral component of aircraft position
$\mathbf{y}$	output vector

Greek letters

α	angle-of-attack
α_i	coefficient
β	angle-of-sideslip
$\boldsymbol{\delta}$	input vector
δ_a	aileron deflection
δ_e	elevator deflection
δ_r	rudder deflection
θ	pitch angle
ξ	transfer function zero
$\boldsymbol{\nu}$	auxiliary input vector
π_{wo}	wash-out pole
ϕ	roll angle
ψ	yaw angle

Subscripts

c	commanded
d	desired

1.0 INTRODUCTION

For hundreds of years flocks of migratory birds have experienced formation flight benefits in terms of improved aerodynamic efficiency, resulting from the upwash vortex generated by the wings of the neighbouring birds. In a similar way, shoals of fishes exploit the advantages offered by synchronised swimming to face the oceanic currents. The aeronautic community, drawing inspiration from these natural behaviours, has focused its interest on the formation flight problem, with the goal of translating the drag drop

Paper No. 3367. Manuscript received 6 November 2008, revised version received 4 February 2009, second revision 15 June 2009, accepted 27 July 2009.

https://doi.org/10.1017/S0001924000003274 Published online by Cambridge University Press

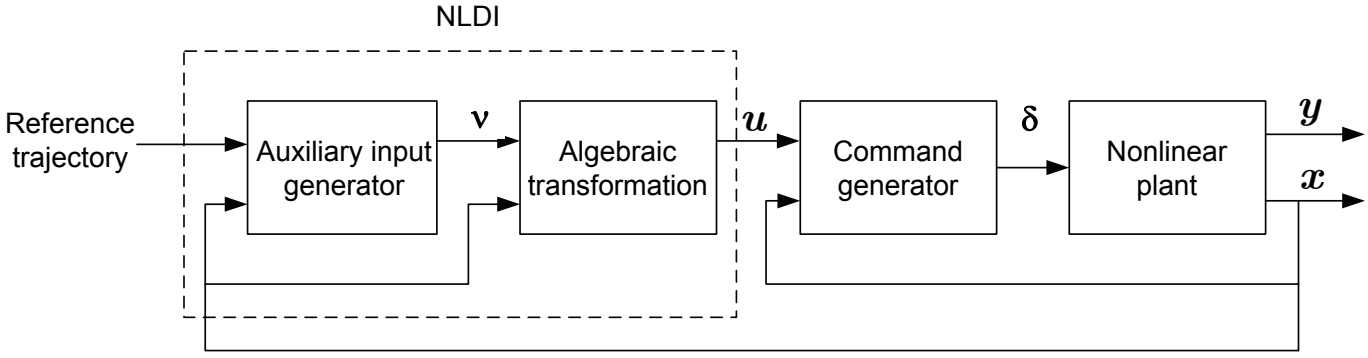


Figure 1. Control system architecture.

concept into a fuel consumption reduction, a very interesting feature especially for long range missions. The main attraction of a formation flight lies not only in the possibility of saving fuel, but also in a number of other applications that are connected with the concepts of formation reconfigurability and coverage capability of selected areas. A further advantage closely related to the employment of unmanned aircraft is the risk removal of human life losses. Due to the above interesting features and the belief that formations of aircraft will play a fundamental role in a near future aerospace scenario, a number of multidisciplinary studies have been conducted on this topic. In particular, from the control system point of view, the challenge is to design a system able to maintain a desired formation geometry. In recent years, Pachter and D'Azzo have carried out a number of works[1-5] concerning the control of close formations (that is, formations in which the lateral separation between aircraft is less than a wingspan). In the first papers the interest was focused in developing two-dimensional control systems for a two-aircraft formation, based on linear, first order autopilots. Afterwards, more complex control systems have been considered, aiming at maintaining a three-dimensional formation geometry. However, the aircraft vertical dynamics has never been explicitly included into the control system. Boskovic and others[6,7] have studied adaptive control algorithms for two-dimensional formation aircraft. Recently, Campa *et al*[8-13] at West Virginia University (WVU) have accomplished interesting studies on the formation flight control problem by analysing a cluster of unmanned aircraft models. In particular, after the identification phase of a nonlinear mathematical model for the WVU YF-22 Aircraft, a nonlinear dynamics inversion (NLDI) based control system has been synthesized. The control system developed by Campa *et al* uses the simplified assumption of two-dimensional formation dynamics. In this paper our aim is to generalise the approach to more complex problems and to extend the results to a three-dimensional geometry.

2.0 BASICS OF NONLINEAR DYNAMIC INVERSION THEORY

To better understand the methodology used in the control system design, it is useful to briefly summarise the main aspects of NLDI theory. The fundamental idea consists in algebraically transforming a nonlinear system into a linear one in such a way that the latter may be controlled with classical methodologies. More precisely, consider a system described in mathematical terms as

$$\begin{aligned}\dot{\mathbf{x}}(t) &= \mathbf{f}(\mathbf{x}(t)) + \mathbf{G}(\mathbf{x}(t))\mathbf{u}(t)\\ \mathbf{y}(t) &= \mathbf{h}(\mathbf{x}(t))\end{aligned} \qquad \ldots (1)$$

where t is the time, $\mathbf{x} \in R^n$ is the state vector, $\mathbf{u} \in R^m$ is the input vector, $\mathbf{y} \in R^m$ is the output vector, $\mathbf{f} \in R^{m\times n}$, $\mathbf{G} \in R^{m\times m}$ and $\mathbf{h} \in R^m$. In accordance to Ref. 14 a square system is assumed, that is, a system with the same number of inputs and outputs. In essence, the NLDI theory suggests to differentiate each output y_j (with j =1, ..., m) with respect to t a sufficient number of times until at least one input appears explicitly in the output equation and the following form is obtained

$$\mathbf{Y}^{\rho} = \mathbf{D}(\mathbf{x}) + \mathbf{E}(\mathbf{x})\mathbf{u} \qquad \ldots (2)$$

where $\mathbf{D} \in R^m$ and $\mathbf{E} \in R^{m\times n}$ (for the sake of compactness, the explicit time dependence has now been omitted). Also

$$\mathbf{Y}^{\rho} \triangleq \left[y_1^{(r_1)},\ldots,y_m^{(r_m)}\right]^T \qquad \ldots (3)$$

where $y_j^{(r_j)} \triangleq \mathrm{d}^{(r_j)} y_j / \mathrm{d}t^{(r_j)}$ and r_1, ..., r_m are suitable integer numbers. Provided that the matrix $\mathbf{E}(\mathbf{x})$ is nonsingular, the algebraic transformation:

$$\mathbf{u} = -\mathbf{E}(\mathbf{x})^{-1}\mathbf{D}(\mathbf{x}) + \mathbf{E}(\mathbf{x})^{-1}\boldsymbol{\nu} \qquad \ldots (4)$$

allows one to recover the following linear and decoupled system:

$$\begin{bmatrix} y_1^{(r_1)} \\ \vdots \\ y_m^{(r_m)} \end{bmatrix} = \begin{bmatrix} \nu_1 \\ \vdots \\ \nu_m \end{bmatrix} \qquad \ldots (5)$$

where the vector $\boldsymbol{\nu} = [\nu_1, \ldots, \nu_m]^T$ plays the role of an auxiliary input. The system (Equation (5)) can be controlled through standard linear techniques.

3.0 MATHEMATICAL MODEL

The NLDI approach has been used to synthesise a control system able to guarantee the trajectory tracking for a formation of autonomous flight vehicles. Although a number of different formation structures have been proposed in the literature[3,5,15,16,17], for the sake of simplicity here we use the so called leader-follower formation geometry. In such a formation type, while the leader maintains a prescribed trajectory, the other aircraft create a chain and each vehicle refers its position to the aircraft directly ahead. For this reason we confine our study to the dynamic behaviour of two aircraft only, as the extension to larger formations does not present any conceptual difference.

By assumption, the whole leader trajectory (in terms of position, velocity and acceleration) is known. This amounts to stating that the desired follower trajectory is given, because the two aircraft are

https://doi.org/10.1017/S0001924000003274 Published online by Cambridge University Press

required to maintain a fixed geometry. The aim of the formation flight control system is to guarantee the trajectory tracking capability over a wide range of flight regimes, as, for example, for different initial conditions of the two aircraft, and for arbitrary flying paths and leader manoeuvres. Moreover, when the prescribed geometry is reached, the two aircraft must be able to maintain the given relative position.

To clarify the discussion, the whole system architecture is first briefly described with the aid of the block diagram shown in Fig. 1.

The generic aircraft in the chain is modelled through nonlinear flight dynamics equations, with input vector $\boldsymbol{\delta} = [T, \delta_e, \delta_a, \delta_r]^T$ and output vector $\mathbf{y} = [x,y,h]^T$. The state vector, which is assumed to be fully measurable, is

$$\mathbf{x} = [V, \quad \alpha, \quad \beta, \quad p, \quad q, \quad r, \quad \psi, \quad \theta, \quad \phi, \quad x, \quad y, \quad h]^T \quad \ldots (6)$$

The aircraft dynamics model is constituted by 12 first order nonlinear differential equations, commonly used to describe the motion of a rigid aircraft flying over a non-rotating and flat Earth[18]. The command generator block uses the information from both the measured state and the intermediate input vector **u** (to be defined below) to provide the current value of the input command. The nonlinear plant and the command generator block form the inner loop of the system, whose dynamics is substantially faster than that of the outer loop. The latter represents the core of the algorithm and is based on a NLDI formulation. In particular, a first block (the auxiliary input generator block) is used for converting the reference trajectory into the current value of auxiliary input **ν**. The latter is then transformed in the intermediate input vector **u** according to the scheme summarised by Equation (4). The various subsystems are analysed in depth in the next sections.

4.0 OUTER LOOP: NLDI CONTROL SYSTEM

The aim of the outer loop is to provide, at each time instant, the current value of intermediate input vector which will be used by the command generator to find the required value of aircraft input command. The components of **u**, that have been chosen both on a mathematical and a physical basis, are the engine thrust T, the time derivative of the pitch angle $\dot{\theta}$ and the time derivative of the roll angle $\dot{\phi}$, that is

$$\mathbf{u} = [T, \dot{\phi}, \dot{\theta}]^T \quad \ldots (7)$$

These variables are used to control, respectively, the longitudinal, lateral and vertical displacements of each aircraft in the formation. As suggested by the NLDI theory, the system output has been differentiated twice with respect to the time. The resulting expressions have been obtained with lengthy calculations and are not shown here for the sake of conciseness. Each expression can be formally written as:

$$\ddot{y}_i = c_{i1}(\mathbf{x}) + c_{i2}(\mathbf{x})T + c_{i3}(\mathbf{x})\dot{\phi} + c_{i4}(\mathbf{x})\dot{\theta} \quad \ldots (8)$$

where y_i stands for the generic component of the output vector **y**. Equation (8) can be rewritten as:

$$\ddot{\mathbf{y}} = \mathbf{D}(\mathbf{x}) + \mathbf{E}(\mathbf{x})\mathbf{u} \quad \ldots (9)$$

which is in the form of Equation (2). The algebraic transformation (4) provides the linearised system:

$$\begin{bmatrix} \ddot{x} \\ \ddot{y} \\ \ddot{h} \end{bmatrix} = \begin{bmatrix} \nu_1 \\ \nu_2 \\ \nu_3 \end{bmatrix} \quad \ldots (10)$$

Equation (10) requires that **E** be invertible, a condition which may be shown to be equivalent to guaranteeing that the term

$$V \cos\alpha \cos\beta \left(\sin\beta \sin\phi + \cos\phi \cos\beta \sin\alpha\right)$$

is non-zero. Accordingly, the singular conditions are characterised by $\alpha = 0$ and either $\beta = 0$ or $\phi = 0$. However, the invertibility problem can be overcome by taking into account the simplifications in the equations of motion that correspond to the occurrence of the above particular values of α, β and ϕ. In practice, the approach is to use different transformations in the form of Equation (10) to cover both the general case and each singular condition (characterised by reduced dynamics). More precisely, at each time instant, and for a given tolerance $\varepsilon > 0$, the control logic checks if $|\alpha| < \varepsilon \cap |\beta| < \varepsilon$ (Case 1), or $|\alpha| < \varepsilon \cap |\phi| < \varepsilon$ (Case 2), or $|\alpha| < \varepsilon \cap |\beta| < \varepsilon \cap |\phi| < \varepsilon$ (Case 3). A suitable control switch associates each case to the proper dynamics, thus automatically avoiding the occurrence of any singularity.

We are now in a position to solve the trajectory tracking problem. Recall that, by assumption, the reference trajectory is given in terms of desired position, velocity and acceleration corresponding to the leader's flight trajectory. Consider, for example, the first component of the output vector and define the error between the actual and desired (subscript d) position as

$$e_x(t) \triangleq x(t) - x_d(t) \quad \ldots (11)$$

Using a command generator tracker approach[18], the error dynamics is required to satisfy the equation

$$\ddot{e}_x(t) + \alpha_{x1}\dot{e}_x(t) + \alpha_{x0}e_x(t) = 0 \quad \ldots (12)$$

where α_{x0} and α_{x1} are suitable positive coefficients. The error dynamics is, therefore

$$\ddot{x}(t) - \ddot{x}_d(t) + \alpha_{x1}\left[\dot{x}(t) - \dot{x}_d(t)\right] + \alpha_{x0}[x(t) - x_d(t)] = 0 \quad \ldots (13)$$

Substituting Equation (10) into (13), yields:

$$\nu_1(t) = \ddot{x}_d(t) - \alpha_{x1}\left[\dot{x}(t) - \dot{x}_d(t)\right] - \alpha_{x0}[x(t) - x_d(t)] \quad \ldots (14)$$

which provides the actual value of auxiliary variable. Clearly, the other two components of vector **ν**, that is, ν_2 and ν_3, are immediately obtained in a similar way. The coefficients α_1 in Equation (14) can be suitably tuned with a trial and error procedure. Table 1 summarises the values used in the succeeding numerical simulations.

Table 1
Coefficients of the error dynamics

x channel	$\alpha_{x0} = 0{\cdot}1$	$\alpha_{x1} = 0{\cdot}01$
y channel	$\alpha_{y0} = 0{\cdot}1$	$\alpha_{y1} = 0{\cdot}01$
h channel	$\alpha_{h0} = 0{\cdot}1$	$\alpha_{hx1} = 0{\cdot}05$

Finally, Equation 4 allows one to calculate the intermediate input **u** that have to be tracked to maintain the formation geometry. Figure 2 summarises the whole procedure.

5.0 INNER LOOP: COMMAND GENERATOR

The intermediate input **u** must be converted into physical inputs for the aircraft. This task is left to the inner loop, whose aim is to generate the time histories of the input vector. With reference to the command generator block of Fig. 1, we will now append a subscript c to the components of vector **u**, to emphasise the differences between commanded variables (with subscript) and measured state

https://doi.org/10.1017/S0001924000003274 Published online by Cambridge University Press

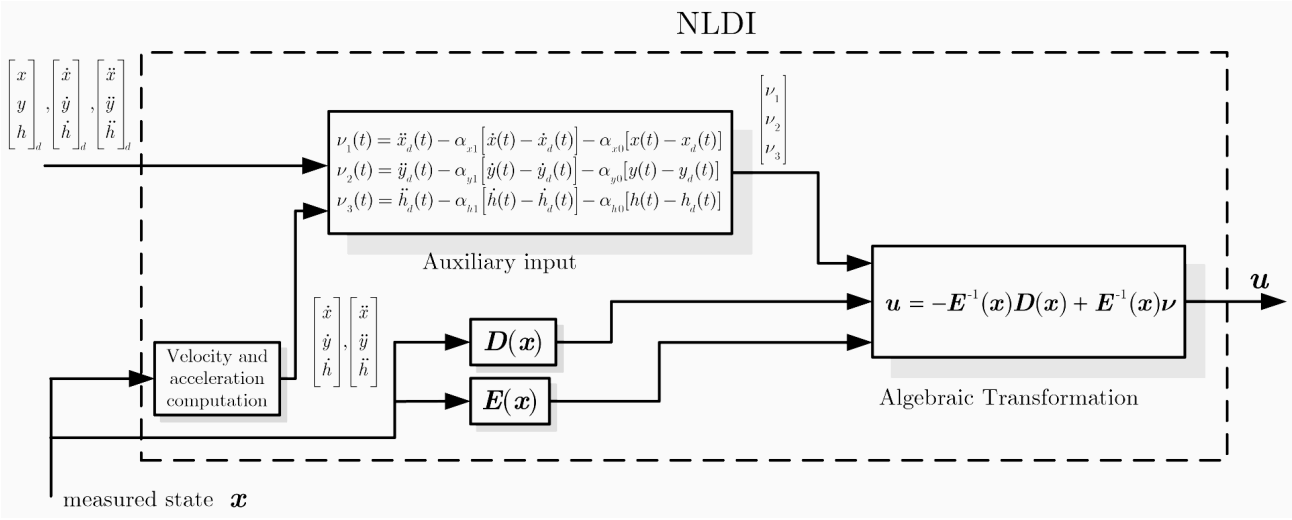


Figure 2. NLDI block diagram.

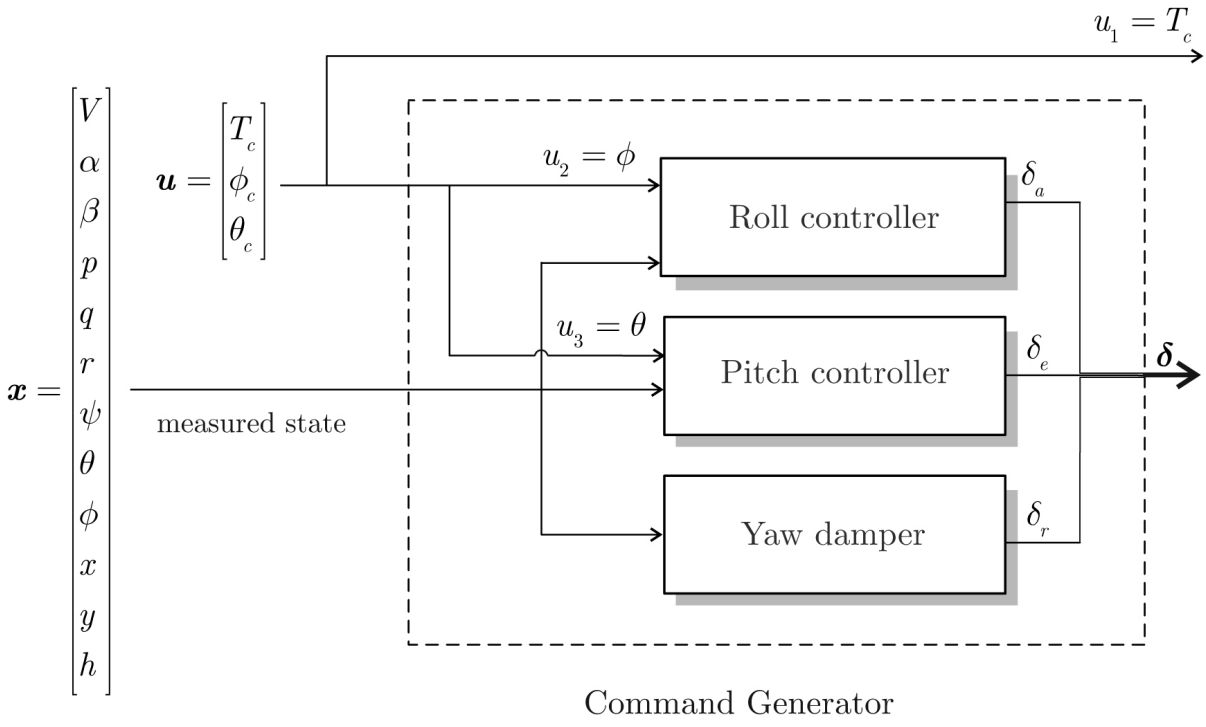


Figure 3. Command generator block diagram.

variables (without any subscript). Bearing in mind Equation 7, the components of **u** are T_c, $\dot{\phi}_c$, and $\dot{\theta}_c$. It is advisable to introduce the commanded angular velocities p_c and q_c with the aid of the following relationships:

$$p_c = \dot{\phi}_c - \dot{\psi}\mathrm{Sin}\theta \quad \ldots (15)$$

$$q_c = \dot{\theta}_c \mathrm{Cos}\,\phi + \dot{\psi}\,\mathrm{Cos}\theta\,\mathrm{Sin}\phi \quad \ldots (16)$$

The first component of **u** is set equal to the corresponding first component of **δ**, that is, $T_c = T$. Moreover, the elevator is used to track $\dot{\theta}$, whereas the aileron deflection is used to track $\dot{\phi}$. The rudder surface does not directly contribute to the tracking but it is used in the design of a yaw damper to improve the aircraft dynamics. The

https://doi.org/10.1017/S0001924000003274 Published online by Cambridge University Press

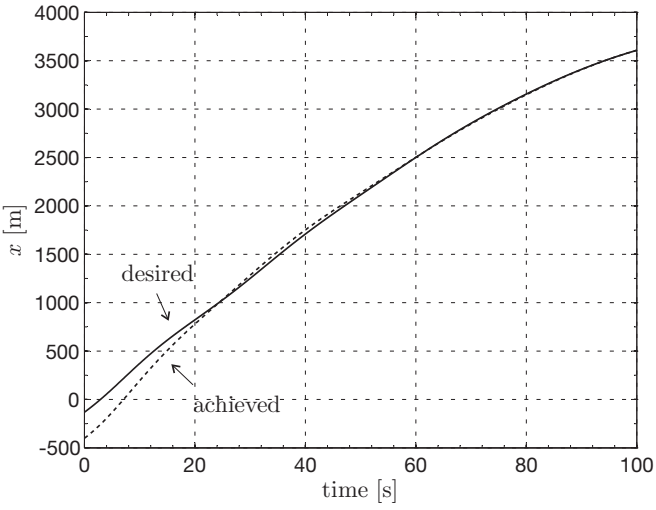


Figure 4. Time history simulation of tracking along *x* axis.

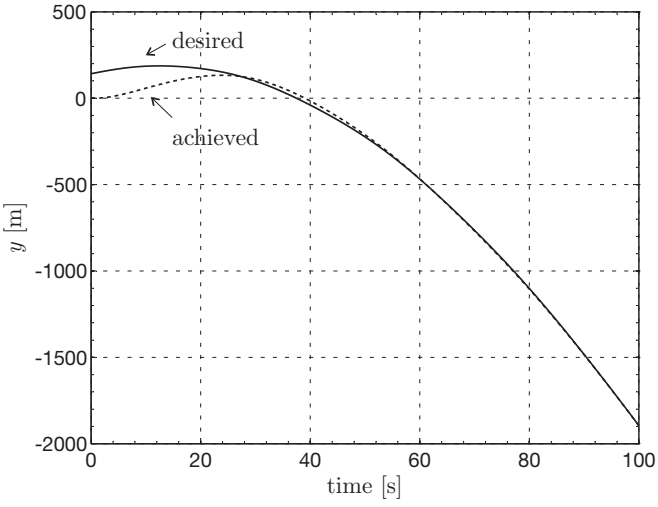


Figure 5. Time history simulation of tracking along *y* axis.

conversion from intermediate to physical inputs is obtained by first deriving an aircraft linearised model. This step allows the designer to exploit the long ripened experience in the field of classical flight control systems where general methodologies are well established. Accordingly, each control system has then been synthesised using a root locus approach, whose main requirement was that of obtaining a fast and damped response. In particular, the longitudinal control is in the form of a proportional-integral controller

$$\delta_e = \frac{k_e(s+\xi_e)}{s}(q-q_d) \qquad \ldots (17)$$

where s is the Laplace variable, k_e is the gain and $-\xi_e$ is the transfer function zero. In a similar way, as far as the lateral control system is concerned, an integral controller is sufficient, that is

$$\delta_a = \frac{k_a}{s}(p-p_d) \qquad \ldots (18)$$

Finally, the stability augmentation system for the rudder channel is

$$\delta_r = \frac{k_r s}{(s+\pi_{wo})}r \qquad \ldots (19)$$

where $-\pi_{wo}$ is the wash-out pole. Figure 3 illustrates the command generator block diagram.

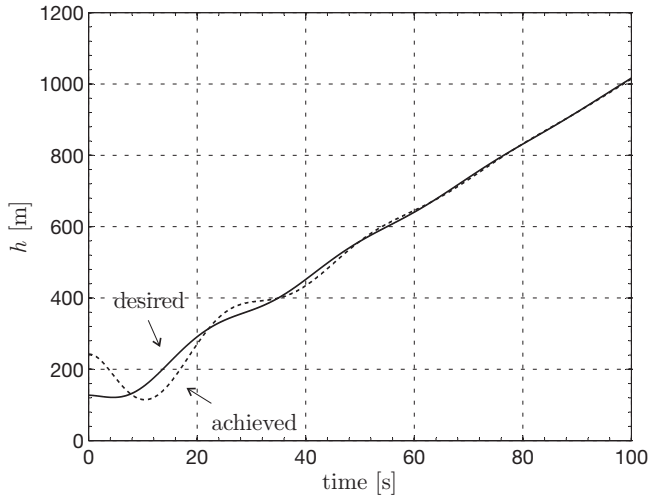


Figure 6. Time history simulation of tracking along *z* axis.

6.0 SIMULATION RESULTS

The above described procedure has been implemented in a Simulink environment and a number of simulations have been performed to demonstrate the control system effectiveness. The reference aircraft in the simulations is the YF-22 reduced-scale prototype developed at West Virginia University, whose main geometrical, inertial and aerodynamic characteristics are described in Refs 8-13. In particular, the aircraft model has a wing span b = 1·96m, a wing aerodynamic chord $\bar{c}$ = 0·76m and a total mass m = 20·64kg. The aircraft aerodynamic model has been summarised in the Appendix. The elevator, aileron and rudder actuators are modelled with first order transfer functions with a time constant τ_δ= 0·04s. The engine is modelled with a first order system too but with a time constant τ_e= 0·25s.

The inner loop has been synthesised with a root locus approach and is characterised by a longitudinal controller with k_e = 0·15s and ξ_e = 10·87s^{-1}, a lateral controller with k_a = 0·55, and a yaw damper with k_r = 0·13s and π_{wo} =1·8s^{-1}.

As a first example, consider a leader-follower formation flight at a trim height of 1,000m and a Mach number of 0·2. Assume an initial position error between the two aircraft given by e_x = 268·6m, e_y = 141·8m and e_h = 115·2m. Figures 4, 5 and 6 show the time histories of both aircraft along x, y and z axes. The position errors are recovered with similar time constants along the three axes and are reduced to negligible values in about 40s.

Also, it should be noted that the NLDI controller is capable of guaranteeing a perfect tracking of the leader trajectory. The corresponding time histories of the commanded inputs, illustrated in Figs 7, 8, 9 and 10, are compatible with the actuator capabilities.

To investigate the robustness characteristics of the control system we now include the presence of uncertainties in the aircraft dynamics model. In particular, each aerodynamic derivative is assumed to exhibit an uncertainty level of 10% with respect to its nominal value. A number of numerical simulations have been conducted using a Monte Carlo approach, and the worst case performance has been found. Figures 11, 12 and 13 show the corresponding worst case simulations. The aircraft position time histories show a qualitative behaviour close to that obtained in the nominal case, and previously illustrated in Figs 4, 5 and 6. More important, the time constant of the error dynamics is similar to the nominal case. As a result, the Monte Carlo analysis substantiates a good robustness level of the whole control system.

https://doi.org/10.1017/S0001924000003274 Published online by Cambridge University Press

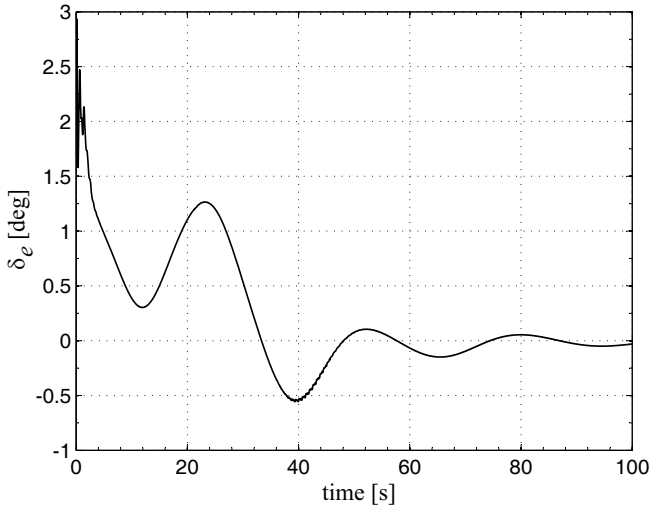


Figure 7. Time history of elevator command.

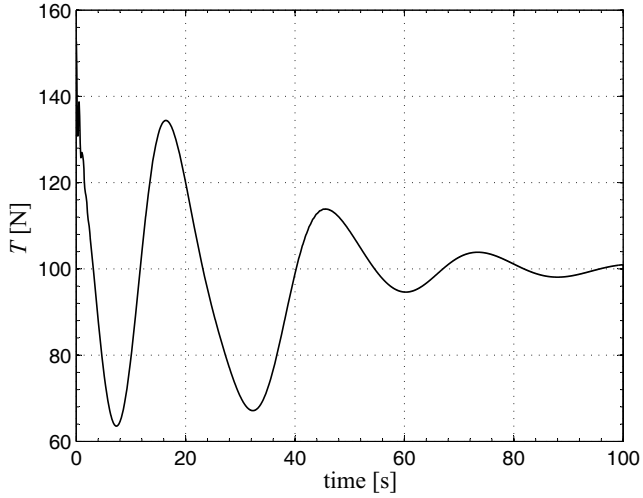


Figure 10. Time history of thrust command.

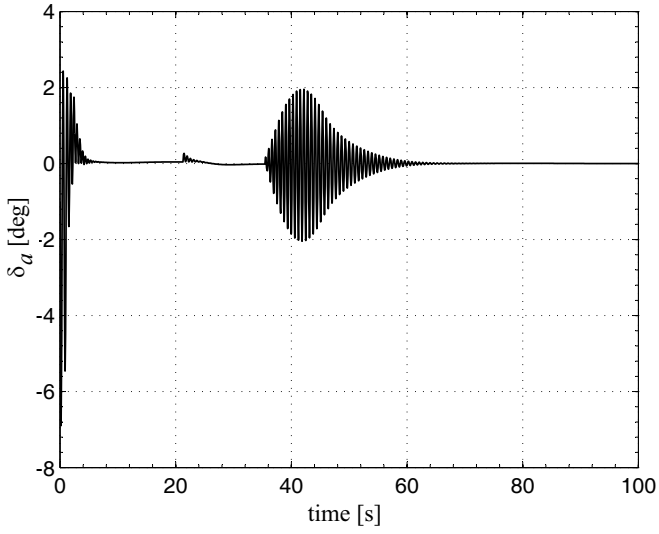


Figure 8. Time history of aileron command.

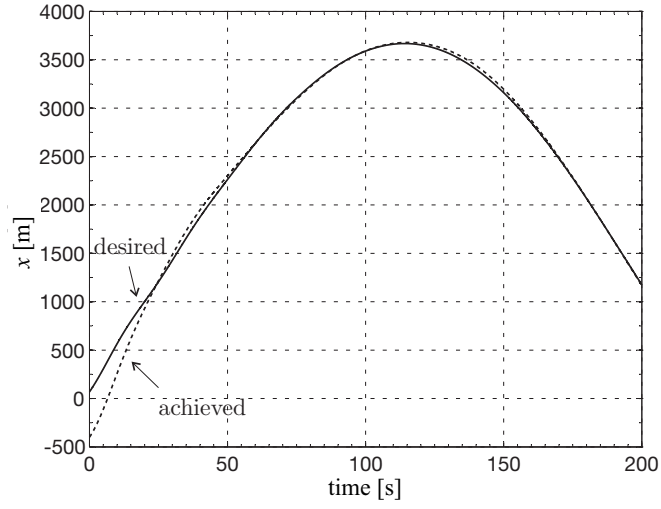


Figure 11. Worst case performance simulation along x axis with aerodynamic uncertainties.

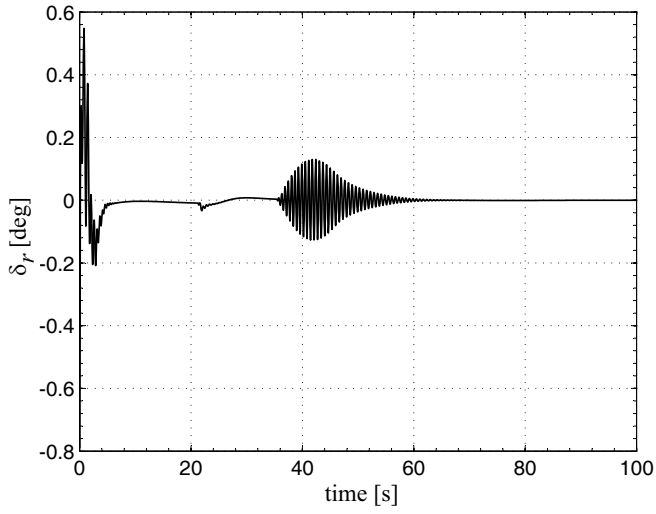


Figure 9. Time history of rudder command.

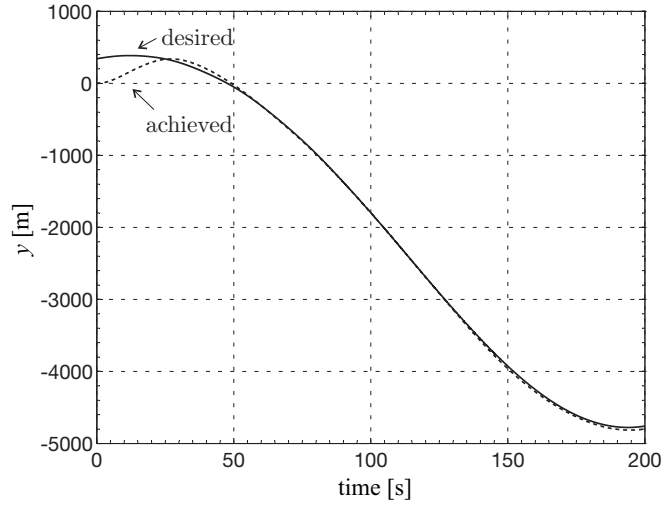


Figure 12. Worst case performance simulation along y axis with aerodynamic uncertainties.

https://doi.org/10.1017/S0001924000003274 Published online by Cambridge University Press

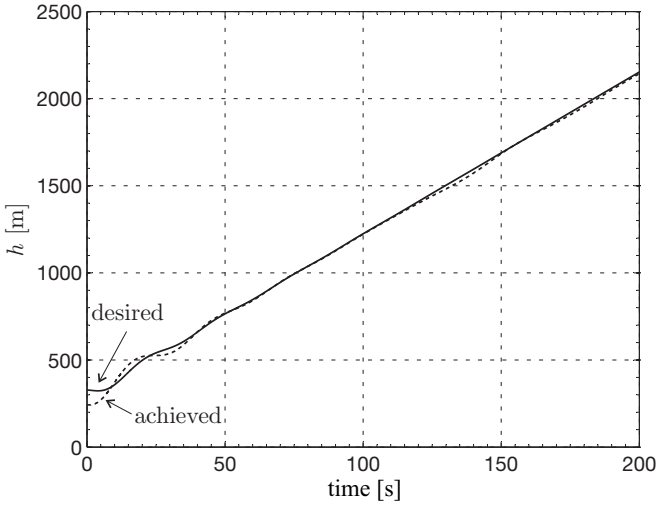


Figure 13. Worst case performance simulation along *z* axis with aerodynamic uncertainties.

7.0 CONCLUSIONS

We have presented the main characteristics of a flight control system, based on a nonlinear dynamic inversion approach, whose aim is to maintain a leader-follower based formation of unmanned aerial vehicles. The whole system architecture is composed of two main loops with different time scale dynamics. While the inner loop provides the commanded input vector, the outer loop uses a NLDI approach to guarantee that the follower aircraft can track the leader's trajectory with zero steady state error. The proposed algorithm exploits a three dimensional formulation of the formation geometry and extends previous results available in the literature. The system performance has been verified with an exhaustive number of simulations in which the aircraft dynamics is described by means of nonlinear equations of motion with realistic inertial and aerodynamic data. The simulations have shown excellent system performance even in presence of significant model uncertainties, thus implying a good level of control system robustness.

REFERENCES

1. BUZOGANY, L.E., PACHTER, M. and D'AZZO, J.J. Automated control of aircraft in formation flight, 1993, AIAA Guidance, Navigation and Control Conference, Monterey, CA, August 1993, pp 1349-1370.
2. PACHTER, M., D'AZZO, J.J. and DARGAN, J.L. Automatic formation flight control, *J Guidance, Control and Dynamics*, November-December 1994, **17**, (6), pp 1380-1383.
3. PROUD, A.W., PACHTER, M. and D'AZZO, J.J. Close formation flight control, 1999, AIAA Guidance, AIAA Paper 99-4207, Navigation and Control Conference, Portland, OR, August 1999.
4. SINGH, S.N., CHANDLER, P., SCHUMACHER, C., BANDA, S. and PACHTER, M. Nonlinear adaptive close formation control of unmanned aerial vehicles, *Dynamics and Control*, April 2000, **10**, (2), pp 179-194.
5. PACHTER, M., D'AZZO, J.J. and PROUD, A.W. Tight formation flight control, *J Guidance, Control and Dynamics*, March-April 2001, **24**, (2), pp 246-254.
6. SAI-MING, L., BOSKOVIC, J.D. and MEHRA, R. Globally stable automatic formation flight control in two-dimensions, 2001, Vol AIAA 2001-4046, AIAA Guidance, Navigation and Control Conference and Exhibition, Montreal, Canada, 6-9 August 2001.
7. BOSKOVIC, J.D., SAI-MING, L. and MEHRA, R.K. Formation flight control design in the presence of unknown leader commands, 2002, American Control Conference Anchorage, AK, 8-10 May 2002.
8. WAN, S., CAMPA, G., NAPOLITANO, M., SEANOR, B. and GU, Y. Design of formation control laws for research aircraft models, 2003, AIAA Paper 2003-5730, AIAA Guidance, Navigation, and Control Conference and Exhibition, Austin, Texas, 11-14 August 2003.
9. CAMPA, G., NAPOLITANO, M.R., SEANOR, B. and PERHINSCHI, M.G. Design of control laws for maneuvered formation flight, 2004, American Control Conference, Boston, Massachusetts, 2004.
10. SEANOR, B., CAMPA, G., GU, Y., NAPOLITANO, M., ROWE, L. and PERHINSCHI, M. Formation flight test results for UAV research aircraft models, 2004, AIAA 1st Intelligent Systems Technical Conference, Chicago, IL, 20-22 September 2004.
11. CAMPA, G., SEANOR, B., GU, Y. and NAPOLITANO, M.R. NLDI guidance control laws for close formation flight, 2005, American Control Conference, Portland, OR, USA, 2005.
12. GU, Y., SEANOR, B., CAMPA, G., NAPOLITANO, M.R., ROWE, L., GURURAJAN, S. and WAN, S. Design and flight testing evaluation of formation control laws, IEEE Transactions on Control Systems Technology, November 2006, **14**, pp 1105-1112.
13. SEANOR, B., GU, Y., NAPOLITANO, M. R., CAMPA, G., GURURAJAN, S. and ROWE, L. Three-aircraft formation flight experiment, 2006, 14th Mediterranean Conference on Control and Automation, 2006.
14. SLOTINE, J.J. and LI, W. *Applied Nonlinear Control*, Chapter 6, 1991, Prentice-Hall, pp 262-272.
15. POLLINI, L. and INNOCENTI, M. A Synthetic environment for dynamic systems control distributed simulation, IEEE control systems magazine, **20**, (2), pp 34-44.
16. ANDERSON, M.R. and ROBBINS, A.C. Formation flight as a cooperative game, 1998, AIAA Guidance, Navigation and Control Conference, AIAA Paper 98-4124, Philadelphia, PA, August 1998.
17. GIULIETTI, F. and MENGALI, G. Dynamics and control of different aircraft formation structures, *Aeronaut J*, March 2004, **108**, (1081), pp 117-124.
18. STEVENS, B.L. and LEWIS, F.L. *Aircraft Control and Simulation*, 1992, John Wiley & Sons, New York.

A1 APPENDIX: AERODYNAMIC MODEL

The aerodynamic forces and moments acting on the aircraft model are, as usual[18]

$$D = \bar{q}SC_D, \quad L = \bar{q}SC_L, \quad Y = \bar{q}SC_Y \qquad \ldots (20)$$

$$\bar{L} = \bar{q}SbC_l, \quad M = \bar{q}S\bar{c}C_M, \quad N = \bar{q}SbC_N \qquad \ldots (21)$$

where D, L and Y are drag, lift and side-force, L, M and N are rolling, pitching and yawing moments and $\bar{q}$ is the dynamic pressure. The aerodynamic coefficients are calculated using the following expressions:

$$C_D = C_{D_0} + C_{D_\alpha}\alpha + C_{D_q}\frac{\bar{c}q}{V} + C_{D_{\delta_e}}\delta_e \qquad \ldots (22)$$

$$C_L = C_{L_0} + C_{L_\alpha}\alpha + C_{L_q}\frac{\bar{c}q}{V} + C_{L_{\delta_e}}\delta_e \qquad \ldots (23)$$

$$C_Y = C_{Y_0} + C_{Y_\beta}\beta + C_{Y_p}\frac{pb}{2V} + C_{Y_r}\frac{rb}{2V} + C_{Y_{\delta_r}}\delta_r + C_{Y_{\delta_a}}\delta_a \qquad \ldots (24)$$

$$C_l = C_{l_0} + C_{l_\beta}\beta + C_{l_p}\frac{pb}{2V} + C_{l_r}\frac{rb}{2V} + C_{l_{\delta r}}\delta_r + C_{l_{\delta a}}\delta_a \qquad \ldots (25)$$

$$C_m = C_{m_0} + C_{m_\alpha}\alpha + C_{m_q}\frac{\bar{c}q}{V} + C_{m_{\delta e}}\delta_e \qquad \ldots (26)$$

$$C_n = C_{n_0} + C_{n_\beta}\beta + C_{n_p}\frac{pb}{2V} + C_{n_r}\frac{rb}{2V} + C_{n_{\delta r}}\delta_r + C_{n_{\delta a}}\delta_a \qquad \ldots (27)$$

https://doi.org/10.1017/S0001924000003274 Published online by Cambridge University Press

Table 2
Longitudinal aerodynamic derivatives

C_{D_0}	=	0·08
C_{D_α}	=	0·508rad^{-1}
C_{D_q}	=	0
$C_{D_{\delta e}}$	=	–0·0339rad^{-1}
C_{L_0}	=	–0·049
C_{L_α}	=	3·258rad^{-1}
C_{L_q}	=	0
$C_{L_{\delta e}}$	=	0·189rad^{-1}
C_{m_0}	=	0·0226
C_{m_α}	=	–0·4738rad^{-1}
C_{m_q}	=	–3·448rad^{-1}
$C_{m_{\delta e}}$	=	–0·3644rad^{-1}

The numerical values of the aerodynamic derivatives are summarised in Tables 2 and 3.

Table 3
Lateral-directional aerodynamic derivatives

C_{Y_0}	=	0
C_{Y_β}	=	0·2725rad^{-1}
C_{Y_p}	=	1·2151rad^{-1}
C_{Y_r}	=	–1·1618rad^{-1}
$C_{Y_{\delta a}}$	=	0·1836rad^{-1}
$C_{Y_{\delta r}}$	=	–0·4592rad^{-1}
C_{l_0}	=	0
C_{l_β}	=	–0·0380rad^{-1}
C_{l_p}	=	–0·2134rad^{-1}
C_{l_r}	=	0·1147rad^{-1}
$C_{l_{\delta a}}$	=	–0·0559rad^{-1}
$C_{l_{\delta r}}$	=	0·0141rad^{-1}
C_{n_0}	=	0
C_{n_β}	=	0·0361rad^{-1}
C_{n_p}	=	–0·1513rad^{-1}
C_{n_r}	=	–0·1958rad^{-1}
$C_{n_{\delta a}}$	=	–0·0358rad^{-1}
$C_{n_{\delta r}}$	=	–0·0555rad^{-1}

https://doi.org/10.1017/S0001924000003274 Published online by Cambridge University Press